

Anharmonic Rice-Ramsperger-Kassel-Marcus (RRKM) and product branching ratio calculations for the partially deuterated protonated water dimers: Dissociation and isomerization

Di Song,¹ Hongmei Su,^{1,a)} Fan-ao Kong,¹ and Sheng-Hsien Lin^{2,3}

¹Beijing National Laboratory for Molecular Sciences (BNLMS), Institute of Chemistry, Chinese Academy of Sciences, Beijing 100190, People's Republic of China

²Institute of Applied Chemistry, Institute of Molecular Science, Chiao-Tung University, Hsin-Chu, Taiwan

³Institute of Atomic and Molecular Science, Academia Sinica, P.O. Box 23-166, Taipei, Taiwan

(Received 30 October 2012; accepted 20 February 2013; published online 8 March 2013)

Partially deuterated protonated water dimers, $\text{H}_2\text{O} \cdot \text{H}^+ \cdot \text{D}_2\text{O}$, $\text{H}_2\text{O} \cdot \text{D}^+ \cdot \text{HDO}$, and $\text{HDO} \cdot \text{H}^+ \cdot \text{HDO}$, as important intermediates of isotopic labeled reaction of $\text{H}_3\text{O}^+ + \text{D}_2\text{O}$, undergo direct dissociation and indirect dissociation, i.e., isomerization before the dissociation. With Rice-Ramsperger-Kassel-Marcus theory and *ab initio* calculations, we have computed their dissociation and isomerization rate constants separately under the harmonic and anharmonic oscillator models. On the basis of the dissociation and isomerization rate constants, branching ratios of two primary products, $[\text{HD}_2\text{O}^+]/[\text{H}_2\text{DO}^+]$, are predicted under various kinetics models with the harmonic or anharmonic approximation included. The feasible kinetics model accounting for experimental results is shown to include anharmonic effect in describing dissociation, while adopting harmonic approximation for isomerization. Thus, the anharmonic effect is found to play important roles affecting the dissociation reaction, while isomerization rates are shown to be insensitive to whether the anharmonic or harmonic oscillator model is being applied. © 2013 American Institute of Physics. [<http://dx.doi.org/10.1063/1.4794152>]

I. INTRODUCTION

Hydrated hydronium ions, $(\text{H}_2\text{O})_n\text{H}^+$, have received considerable attention since they are involved in aqueous proton transfer which plays important roles in many chemical and biological processes.^{1–15} In an investigation with time-resolved Fourier transform infrared spectroscopy (TR-FTIR) and *in situ* $\text{H}_2^{18}\text{O}/\text{H}_2^{16}\text{O}$ exchange FTIR, Gerwert and co-workers⁵ determined how the membrane protein bacteriorhodopsin uses the interplay among strongly hydrogen-bonded water molecules, a water molecule with a dangling hydroxyl group, and a protonated water cluster to transfer protons. In contrast to this controlled proton transfer in protein environment, a more random proton migration occurs in liquid water through the interconversion between an Eigen cation $(\text{H}_2\text{O})_4\text{H}^+$ and a Zundel cation $(\text{H}_2\text{O})_2\text{H}^+$.^{6,7} The latter, i.e., the protonated water dimer represented by an excess proton equally shared between two water molecules $(\text{H}_2\text{O} \cdots \text{H}^+ \cdots \text{OH}_2)$, has shown to possess quite large anharmonicity because the shared proton vibrates in a rather flat potential and undergoes a large amplitude motion.^{6–11}

Here, we focus our study on partially deuterated protonated water dimers $\text{H}_2\text{O} \cdot \text{H}^+ \cdot \text{D}_2\text{O}$, $\text{H}_2\text{O} \cdot \text{D}^+ \cdot \text{HDO}$, and $\text{HDO} \cdot \text{H}^+ \cdot \text{HDO}$ that are important intermediates of the isotopic labeled reaction of $\text{H}_3\text{O}^+ + \text{D}_2\text{O}$. As an effective method for exploring the proton transfer dynamics, the isotopic labeled reaction of $\text{H}_3\text{O}^+ + \text{D}_2\text{O}$ (shown in Figure 1) can provide a clear physical picture for the proton mi-

gration during the symmetric exchange between two water molecules. Meanwhile, the existence of deuterium atom results in isomerizations among partially deuterated protonated water dimers, which invokes another type of important reaction, isotope scrambling. As shown in the reaction scheme of Figure 1, a proton transfer to form $\text{HD}_2\text{O}^+ + \text{H}_2\text{O}$ mainly occurs via direct dissociation of $\text{H}_2\text{O} \cdot \text{H}^+ \cdot \text{D}_2\text{O}$, while isotope scrambling to form $\text{HD}_2\text{O}^+ + \text{H}_2\text{O}$ requires the three intermediates to live sufficiently long such that they isomerize before their dissociation. Indeed, Rheinecker *et al.*'s¹² theoretical study suggested that the intermediate of $\text{H}_3\text{O}^+ + \text{H}_2\text{O}$ reaction was a long-lived complex. In a crossed-beam study of $\text{H}_3\text{O}^+ + \text{D}_2\text{O}$ reaction, Ryan *et al.*¹³ observed two primary products, HD_2O^+ formed by proton transfer and H_2DO^+ generated from isotope scrambling at a collision energy of 0.7 eV.

The competition between proton transfer *versus* isotope scrambling, as reflected by the product branching ratio of $[\text{HD}_2\text{O}^+]/[\text{H}_2\text{DO}^+]$, strongly relies on dissociation and isomerization rates of the three intermediates. To theoretically describe the competition between proton transfer and isotope scrambling, the key is to obtain the dissociation and isomerization rates. For such protonated water dimers, anharmonic effect is required to be taken into account in principal because of their large anharmonicity. Our earlier work¹⁴ indicated that the anharmonic Rice-Ramsperger-Kassel-Marcus (RRKM) theory could provide a reasonably good description for dissociation rate constants of $(\text{H}_2\text{O})_2\text{H}^+$ and its deuterated analog $(\text{D}_2\text{O})_2\text{D}^+$. However, it remains unclear how anharmonicity affects the isomerization rate constants for this type of systems. Due to the lack of experimental isomerization

^{a)}E-mail: hongmei@iccas.ac.cn.

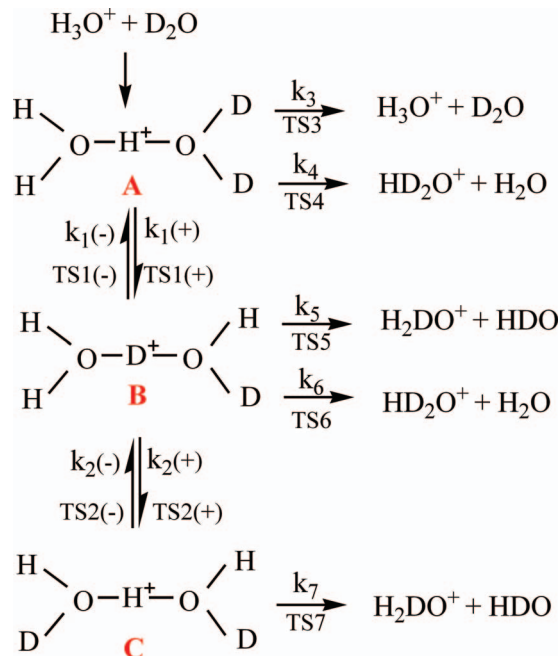


FIG. 1. Reaction scheme of the isotope labeled reaction of $\text{H}_3\text{O}^+ + \text{D}_2\text{O}$.

rates for comparison, it is hard to examine this issue with only the RRKM calculation results. Fortunately, branching ratios of $[\text{HD}_2\text{O}^+]/[\text{H}_2\text{DO}^+]$ as a function of collision energy were measured with the guided-ion beam mass spectrometry,¹⁵ which provides information about the reaction rate competition between dissociation and isomerization and thus allows the calculated results to be compared with.

In this paper, we first compute dissociation and isomerization rate constants for the partially deuterated protonated water dimers $\text{H}_2\text{O} \cdot \text{H}^+ \cdot \text{D}_2\text{O}$, $\text{H}_2\text{O} \cdot \text{D}^+ \cdot \text{HDO}$, and $\text{HDO} \cdot \text{H}^+ \cdot \text{HDO}$ separately under the harmonic and anharmonic oscillator models by using RRKM theory and *ab initio* calculations. On the basis of these obtained harmonic and anharmonic rate constants, the calculations of branching ratios $[\text{HD}_2\text{O}^+]/[\text{H}_2\text{DO}^+]$ as a function of the energy are performed under various kinetics models. Comparison of the calculated branching ratios with the experimental values enables evaluating how important the anharmonicity affects isomerization and dissociation kinetics of partially deuterated protonated water dimers as well as deriving a feasible kinetics model to rationalize the kinetic energy dependence experimentally observed with the product branching ratios of proton transfer versus isotope scrambling.

II. COMPUTATIONAL METHODS

A. RRKM calculation

For a unimolecular reaction $A^* \rightarrow A^\ddagger \rightarrow P$, the rate constant $k(E)$ with an internal energy E is given by the RRKM theory (often called quasi-equilibrium theory) as

$$k(E) = \frac{\sigma W^\ddagger(E - E^\ddagger)}{h \rho(E)}, \quad (1)$$

where σ is the reaction path degeneracy, h is Planck's constant, $\rho(E)$ represents the density of states of the energized reactant molecule A^* , and $W^\ddagger(E - E^\ddagger)$ denotes the total number of states for the activated complex A^\ddagger , whose activation energy is E^\ddagger . In essence, the RRKM theory is a statistical theory, based on the assumption that the rate of intramolecular vibrational energy redistribution is so rapid that the dynamical details are unimportant, and thus all energetically accessible quantum states will be populated equally.

Conventionally, RRKM calculations are performed with the harmonic approximation. The Beyer–Swinehart algorithm used in this work is an effective method to evaluate the state density and state numbers in harmonic RRKM calculations.¹⁶ However, for some systems with the weak bond, such as $(\text{H}_2\text{O})_2\text{H}^+$ and $(\text{HF})_2$, the anharmonic effect is significant.^{14,17–20} Generally speaking, the anharmonic effect on the potential surface has two aspects: One involves the modification of vibrational energy levels (or frequencies) of vibrational modes. Recent studies related to this anharmonic effect have been conducted in the electronic absorption and emission spectra, photophysical processes, unimolecular dissociations of molecules and clusters, and vibrational dynamics of liquid water.^{14,17–22} The other aspect is related to the mode-mode coupling which can induce vibrational relaxation and modify the IR spectra through the appearance of side bands and the broadening of band-widths.^{23,24} The adiabatic approximation model has been proposed to treat this mode-mode coupling effect for obtaining the fine IR spectra (accurate vibrational frequencies).²⁴ In this paper, we mainly use the Morse oscillator to describe the anharmonic effect on the modification of the energy levels which is closely related to the calculation of reaction rate constants. The Morse oscillator model has turned out to be an effective way of treating the anharmonic effect in previous studies.^{14,18–20} The eigenenergy of the Morse oscillator can be expressed by

$$E_{n_i} = \left(n_i + \frac{1}{2}\right) \hbar \omega_i - \chi_i \left(n_i + \frac{1}{2}\right)^2 \hbar \omega_i, \quad (2)$$

where χ_i is the anharmonic constant, ω_i is the frequency of the i th vibrational mode, and n_i is the vibration quantum number of the vibrational mode. Equation (2) accounts well for the anharmonicity of the real bond, since the Morse oscillator energy level spacing decreases as the energy approaches the dissociation energy and the maximum quantum number $n_i(\text{max})$ exists. All the vibrational modes are treated anharmonically using the Morse oscillator model including the reaction coordinate, the O–O bond stretch mode. It should be noted that low frequency vibrations below 100 cm^{-1} are treated separately with internal rotations to improve the accuracy of rate constants. Typically, the anharmonic constants χ_i can be theoretically determined by the second-order perturbation theory approach of Barone,²⁵ or by vibrational self-consistent field methods of Bowman,²⁶ Gerber and Ratner,²⁷ or by the fitting of force constants. In this work, the anharmonic constants are calculated by the second-order perturbation theory approach implemented in GAUSSIAN 03^{25,28} and only the diagonal anharmonic constants are adopted.

In the evaluation of $W^\ddagger(E - E^\ddagger)$ and $\rho(E)$, we continue to use the computational algorithm developed for

implementing direct state counting under the anharmonic model in previous paper.¹⁴ For further improving computational efficiency, the following optimizations for this algorithm are performed in this work. (1) Before counting numbers of combinations, we sort energy level values of each vibrational mode in descending order, respectively. (2) If an effective combination is formed by an energy level of a vibrational mode and corresponding energy levels of other vibrational modes, then combinations obtained by this vibrational energy level and smaller energy levels of other vibrational modes will be all effective. In this case, numbers of these combinations will be directly calculated in light of combinatorics formula, which significantly saves computational time.

B. *Ab initio* calculations and variation transition state theory (VTST)

The properties of the reactant and activated complex are required in RRKM calculations. The geometries of reactants and transition states (TS) in isomerization process are optimized using the MP2 (full) method with 6-311++G (2d, 2p) basis set. Harmonic vibrational frequencies, anharmonic constants, and zero-point energies (ZPE) are calculated at the same calculation level with optimized geometries. Activation energies of the reaction thus are obtained after ZPE correction. All the quantum chemical calculations have been carried out using the GAUSSIAN 03 program.²⁸

It is noticeable that we use the VTST approach to obtain TS of dissociation by considering different positions for the TS along the reaction path, calculating rate constants corresponding to each of them, and finding the minimal value.^{19,20,29} This is because the dissociation of partially deuterated protonated water dimers is a simple bond cleavage process, and no distinct TS exists in the potential energy surfaces (PES). The approach has been described in detail previously, therefore, only a brief summary is given here.¹⁴ The minimal RRKM rate constant corresponding to the variational TS can be obtained along the reaction path q^\ddagger according to the following equation:

$$\frac{dk(E)}{dq^\ddagger} = 0. \quad (3)$$

In other words, the approach calculates rate constants at different positions corresponding different TS along the reaction path until the minimal rate is found. The reaction coordinates in our calculations are chosen as the lengths of breaking O-O bond. Each RRKM calculation requires values of activation energy, ZPE, and vibrational frequencies as function of reaction coordinate.

III. RESULTS AND DISCUSSIONS

A. Quantum chemistry calculation results

$\text{H}_2\text{O} \cdot \text{H}^+ \cdot \text{D}_2\text{O}$, $\text{H}_2\text{O} \cdot \text{D}^+ \cdot \text{HDO}$, and $\text{HDO} \cdot \text{H}^+ \cdot \text{HDO}$ are important intermediates of the isotope labeled reaction of $\text{H}_3\text{O}^+ + \text{D}_2\text{O}$. As shown in Figure 1, $\text{H}_2\text{O} \cdot \text{H}^+ \cdot \text{D}_2\text{O}$, $\text{H}_2\text{O} \cdot \text{D}^+ \cdot \text{HDO}$, and $\text{HDO} \cdot \text{H}^+ \cdot \text{HDO}$ undergo dissociation and isomerization to generate various fragment ions. To ob-

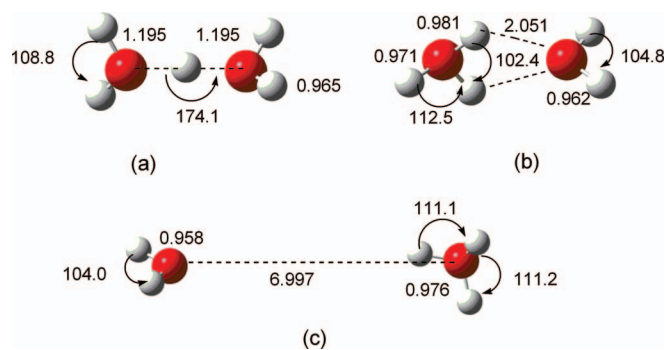


FIG. 2. The optimized geometries of (a) $\text{H}_2\text{O} \cdot \text{H}^+ \cdot \text{D}_2\text{O}$, $\text{H}_2\text{O} \cdot \text{D}^+ \cdot \text{HDO}$, and $\text{HDO} \cdot \text{H}^+ \cdot \text{HDO}$, (b) TS1 and TS2 for the isomerization, and (c) TS3-TS7 for the dissociation. All geometries were obtained with MP2 (full) 6-311++G(2d,2p) calculations. Bond lengths are in angstrom and bond angles are in degree.

tain dissociation and isomerization rate constants, the properties of the reactants and transition states in the reaction process are required to be known first.

In light of Born-Oppenheimer approximation, the partially deuterated protonated water dimers, $\text{H}_2\text{O} \cdot \text{H}^+ \cdot \text{D}_2\text{O}$, $\text{H}_2\text{O} \cdot \text{D}^+ \cdot \text{HDO}$, and $\text{HDO} \cdot \text{H}^+ \cdot \text{HDO}$, are believed to have the same geometry and PES as those of $(\text{H}_2\text{O})_2\text{H}^+$. Accordingly, we performed *ab initio* calculations of the $(\text{H}_2\text{O})_2\text{H}^+$ ion at the level of MP2(full)/6-311++G(2d,2p), and obtained its optimized geometry (Figure 2(a)). Adopting this geometry and considering isotope effect, the harmonic vibrational frequencies and anharmonic constants of the deuterated protonated water dimers were calculated at the same level and the results are summarized in Table I.

The isomerization processes are reversible, corresponding to four TSs. For TS of each isomerization step, the optimized geometry is shown to be a bridged structure by MP2 (full)/6-311++G (2d,2p) calculations (see Figure 2(b)). Such geometry agrees with previous calculation results.^{15,30} After ZPE corrections, isomerization activation energies of TS1(+), TS1(-), TS2(+), and TS2(-) are 12.70, 12.11, 12.75, and 12.77 kcal/mol, respectively. These energies are in agreement with Honma *et al.*'s calculations in which the bridged transition states lie 12.3 kcal/mol above $(\text{H}_2\text{O})_2\text{H}^+$,¹⁵ but differ from Evleth *et al.*'s result because of different calculation method and basis sets applied.³⁰

However, no distinct TS exists for dissociation of these deuterated protonated water dimers because the reverse process (i.e., the combination of hydronium ion and water) is barrierless. In this case, we use the VTST approach to obtain variational TS for each dissociation pathway. The geometry of the TSs is thus obtained and plotted in Figure 2(c). Figure 2(c) shows the TS structure obtained at the collision energy of 31.45 kcal/mol with the VTST method and the TS structure is independent of the energy in the inspected energy range. For $\text{H}_2\text{O} \cdot \text{H}^+ \cdot \text{D}_2\text{O}$, $\text{H}_2\text{O} \cdot \text{D}^+ \cdot \text{HDO}$, and $\text{HDO} \cdot \text{H}^+ \cdot \text{HDO}$, each of the first two can dissociate in two ways, and the last one has only one dissociation channel. Correspondingly, there are five TSs (TS3-TS7) for the dissociation processes. After ZPE correction, the activation energies for dissociation pathway are separately 30.50, 30.37, 30.95, 31.05, and 31.04

TABLE I. Harmonic vibrational frequencies (cm^{-1}) and anharmonic constants calculated at the level of MP2 (full)/6-311++G (2d, 2p). The anharmonic constants are obtained by the second-order perturbation theory approach implemented in GAUSSIAN 03 and the diagonal anharmonic constants are listed.

Ions	Harmonic frequencies	Anharmonic constants
A	153, 258, 391, 453, 542, 606, 771, 1267, 1505, 1648, 1755, 2732, 2855, 3794, 3891	0.0728,0.0520,0.0012,0.0388,0.0077,0.0086,0.0016,0.0068, 0.0387,0.0390,0.0082,0.0088,0.0104,0.0123,0.0137
B	162, 251, 432, 449, 517, 618,658, 1164, 1235, 1520, 1704, 2788, 3793, 3849, 3891	0.0763,0.0122,0.0090,0.0639,0.0237,0.0119,0.0006,0.0386, 0.0508,0.0078,0.0087,0.0169,0.0122,0.0231,0.0137
C	147, 262, 431, 443, 481, 619, 776, 1406, 1497, 1596, 1704, 2785, 2791, 3847, 3851	0.0675,0.0001,0.0476,0.0067,0.0419,0.0046,0.0001,0.0077, 0.033,0.0075,0.0229,0.0081,0.0081,0.0111,0.0111
TS1	-384, 240, 294, 322, 416, 434, 935, 1259, 1485, 1692, 2590, 2738, 3596, 3815, 3911,	0.0054,0.0145,0.0347,0.0059,0.0106,0.0321,0.008,0.0068, 0.0093,0.0121,0.0131,0.023,0.0111,0.0120
TS2	-397, 260, 285, 293, 399, 409, 990, 1416, 1490, 1627, 2612, 2808, 3585, 3746, 3863	0.0058,0.0171,0.0121,0.0071,0.0093,0.0442,0.0042, 0.0067,0.0087,0.0167,0.0156,0.0205,0.0209,0.0216
TS3	-23, 9, 41, 54, 114, 142, 925, 1223, 1715, 1717, 2785, 2914, 3611, 3713, 3721	0.0001,0.2113,0.1637,0.0115,0.0001,0.0894,0.0083,0.0076, 0.0077,0.0080,0.0093,0.0079,0.0119,0.0130
TS4	-23, 10, 31, 46, 157, 189, 778, 1283, 1549, 1672, 2624, 2734, 3677, 3863, 3977	0.0001,0.2008,0.1575,0.005,0.0001,0.0683,0.0038, 0.0065,0.0112,0.0083,0.0100,0.0237,0.0112,0.0121
TS5	-23, 10, 32, 42, 157, 189, 776, 1283, 1547, 1672, 2620, 2730, 3688, 3863, 3977	0.0001,0.2240,0.1107,0.0051,0.0001,0.0683,0.0038, 0.0065,0.0112,0.0083,0.0100,0.0237,0.0112,0.0121
TS6	-23, 9, 37, 43, 131, 168, 853, 1450, 1466, 1691, 2670, 2847, 3653, 3721, 3923	0.0001,0.1912,0.1135,0.0191,0.0001,0.0812,0.0044, 0.009,0.0070,0.017,0.0154,0.0117,0.0130,0.0214
TS7	-23, 9, 34, 51, 131, 168, 855, 1450, 1466, 1692, 2678, 2847, 3648, 3715, 3923	0.0001,0.2324,0.1571,0.0190,0.0001,0.0803,0.0043, 0.0090,0.0070,0.0169,0.0154,0.0120,0.0133,0.0214

kcal/mol. These results are consistent with experimental values of 31.6 and 31.8 kcal/mol and a theoretical value of 30.95 kcal/mol for $(\text{H}_2\text{O})_2\text{H}^+$.^{15,31,32} All the obtained harmonic vibrational frequencies and anharmonic constants for the TSs of the isomerization and dissociation are also collected in Table I.

B. Anharmonic effect on dissociation and isomerization processes

On the basis of the above *ab initio* calculation results, dissociation and isomerization rate constants for these partially deuterated protonated water dimers, $\text{H}_2\text{O} \cdot \text{H}^+ \cdot \text{D}_2\text{O}$, $\text{H}_2\text{O} \cdot \text{D}^+ \cdot \text{HDO}$, and $\text{HDO} \cdot \text{H}^+ \cdot \text{HDO}$, are separately computed under the harmonic oscillator and anharmonic oscillator models within RRKM formalism. The calculated reaction rate constants are listed in Tables S1 and S2,³³ and illustrated in Figure 3, respectively.

For the convenience of discussion, we use A, B, and C to denote $\text{H}_2\text{O} \cdot \text{H}^+ \cdot \text{D}_2\text{O}$, $\text{H}_2\text{O} \cdot \text{D}^+ \cdot \text{HDO}$, and $\text{HDO} \cdot \text{H}^+ \cdot \text{HDO}$ hereafter. For dissociation rate constants (k_3-k_7), as shown in Figure 3(a), harmonic and anharmonic results are close to each other merely in quite low energy range (~ 1 kcal/mol above activation energy). The deviation between harmonic and anharmonic results becomes larger when the total energy rises. Such a big difference is caused by the use of the different models, the harmonic and anharmonic potentials (the Morse potential), to describe the vibrational energy levels in the calculations. The harmonic rate constants always go up with the increasing total energy, because the harmonic RRKM calculations overstate the number of states by using linear quantum harmonic vibration equation. On the contrary, the anharmonic RRKM calculations take into account the effect of Morse potential on the bond breaking so

that anharmonic rate constants tend to reach a plateau as the total energy is increased beyond a certain limit. The calculation results show that the dissociation of A, B, and C exhibits significant anharmonic effect.

From Table S1,³³ it can be also seen that when anharmonic rate constants of A, B, and C approach the limit of 10^{12} s^{-1} , their harmonic rate constants already reach 10^{13} s^{-1} and even 10^{14} s^{-1} in the high energy range (about 50–73 kcal/mol). Obviously, the harmonic results are unreasonable, because the dissociation rate should be smaller than the rate of intramolecular vibrational relaxation (10^{13} – 10^{12} s^{-1}) according to RRKM theory. Therefore, RRKM calculations of dissociation rate constants should take the

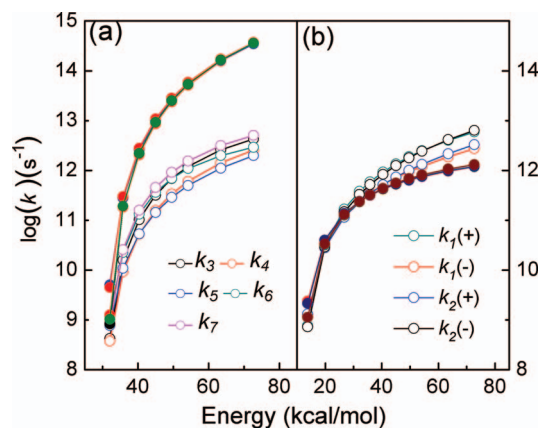


FIG. 3. (a) Dissociation and (b) isomerization rate constants under separately harmonic and anharmonic oscillator models for $\text{H}_2\text{O} \cdot \text{H}^+ \cdot \text{D}_2\text{O}$, $\text{H}_2\text{O} \cdot \text{D}^+ \cdot \text{HDO}$, and $\text{HDO} \cdot \text{H}^+ \cdot \text{HDO}$. Solid dots correspond to harmonic results, where rate constants for each isomerization step or dissociation channel are similar. Hollow dots represent anharmonic results, where rate constants for each isomerization step or dissociation channel are slightly different and are labeled underneath the curves.

anharmonic effect into account, especially in the high energy range. This is consistent with our previous finding for $(\text{H}_2\text{O})_2\text{H}^+$ in which proper description of the dissociation rate constants was only obtained under anharmonic model. The experimentally obtained IR spectra of $(\text{H}_2\text{O})_2\text{H}^+$ revealed vibrational frequencies deviated from harmonic fundamentals, also suggesting considerable anharmonic effect for protonated water dimers.^{9,10}

For isomerization rate constants of A, B, and C, as shown in Figure 3(b), there is almost no difference between harmonic and anharmonic results in the energy range of ~ 13 – 32 kcal/mol. When the energy continues to increase, the deviation between harmonic and anharmonic results is still not large. Even in the high energy range, anharmonic isomerization rate constants are only about two to five times as large as harmonic results. These results indicate that isomerization rates are insensitive to whether anharmonic or harmonic oscillator model is being applied.

It is noticeable that there are three low frequencies (< 100 cm^{-1}) in the dissociation TSs (TS3-TS7), whereas in isomerization TSs (TS1 and TS2), all frequencies are higher than 200 cm^{-1} . In the dissociation process of protonated water dimers, no distinct TS exists. For performing RRKM calculations, we use the VTST approach to obtain the variational TS. Compared to the normal TSs in the isomerization process, the dissociation TSs have very long O-O bond length (about 6.997 Å), inevitably leading to low frequency vibrations. To obtain more accurate dissociation rate constants, these low frequency vibrations below 100 cm^{-1} are separately treated as internal rotations in the calculation of dissociation rate constants, while other frequency vibrations are treated with the anharmonic (Morse oscillator) model. The potential energy barriers for internal rotations related to these three low frequency vibrations are obtained at MP2 (full)/6-311++(2d,2p) level. The calculated barrier heights (E_{rot}) for the three internal rotations are 2 cm^{-1} , 11 cm^{-1} , and 230 cm^{-1} , respectively. Depending on the magnitude of the barriers involved, the low frequency vibrations with $E_{\text{rot}} = 2$ cm^{-1} and 11 cm^{-1} are treated with free internal rotations, and the low frequency vibration with $E_{\text{rot}} = 230$ cm^{-1} is treated with hindered internal rotation. For free internal rotations, the energy levels are calculated by the formalism of $E_m = m^2\hbar^2/2I$ ($m = 0, \pm 1, \pm 2, \dots$). For the hindered internal rotation, the eigenenergies of the rotational potential energy surface are calculated numerically using discrete variable representation method.³⁴ The sum of states of dissociation TSs is estimated by the direct counting method.

The calculated dissociation rate constants under the anharmonic (Morse oscillator) model with free or hindered internal rotations treatment are listed in Table S3,³³ which are about 2–3 times larger than those obtained under pure Morse oscillator treatment (results in Table S1 in the supplementary material³³), and are still in the reasonable range. As will be discussed in Sec. III C, when these dissociation rate constants obtained under the anharmonic model with free or hindered internal rotations treatment are applied in calculating the product branching ratios, more reasonable results in better agreement with experimental results will be obtained.

C. Branching ratios

As shown in Figure 1, there are two primary products, HD_2O^+ and H_2DO^+ formed from the isotope labeled reaction of $\text{H}_3\text{O}^+ + \text{D}_2\text{O}$ through the three intermediates A, B, and C. HD_2O^+ is mainly produced by direct dissociation of A, whereas H_2DO^+ is formed via indirect dissociation, i.e., A isomerizes to B and C followed by respective dissociations. Branching ratio of the two primary products, $[\text{HD}_2\text{O}^+]/[\text{H}_2\text{DO}^+]$, reflects the competition between direct and indirect dissociation after isomerization. The calculated dissociation and isomerization rate constants provide a basis for deriving a kinetics model of branching ratios.

As illustrated in Figure 1, we separately define rate constant for each isomerization step and dissociation channel. Under this kinetics scheme, formation rate of products HD_2O^+ and H_2DO^+ can be written by the following equations:

$$d[\text{HD}_2\text{O}^+]/dt = k_4[A] + k_6[B], \quad (4)$$

$$d[\text{H}_2\text{DO}^+]/dt = k_5[B] + k_7[C]. \quad (5)$$

The kinetics expressions for B and C are given by

$$d[B]/dt = k_1(+)[A] + k_2(-)[C] - M_1[B], \quad (6)$$

$$d[C]/dt = k_2(+)[B] - (k_2(-) + k_7)[C], \quad (7)$$

where $M_1 = k_5 + k_6 + k_2(+)+k_1(-)$. Application of the steady state assumption to intermediates B and C yields

$$[B] = \frac{k_7 + k_2(-)}{k_2(+)} [C], \quad (8)$$

$$[A] = \frac{M_1(k_7 + k_2(-)) - k_2(+k_2(-))}{k_1(+k_2(+))} [C]. \quad (9)$$

Substituting Eqs. (8) and (9) into Eqs. (4) and (5), branching ratio of HD_2O^+ and H_2DO^+ can be expressed as

$$\frac{[\text{HD}_2\text{O}^+]}{[\text{H}_2\text{DO}^+]} = \frac{k_1(+k_6(k_7 + k_2(-)) + k_4(M_1(k_7 + k_2(-)) - k_2(+k_2(-))))}{k_1(+)(k_5(k_7 + k_2(-)) + k_2(+k_7))}. \quad (10)$$

With this kinetics scheme, branching ratios of the two primary products, $[\text{HD}_2\text{O}^+]/[\text{H}_2\text{DO}^+]$, can be calculated under various models as below. One is the Harmonic-Harmonic (H-H) model in which harmonic dissociation and harmonic isomerization rate constants are used in the formula. The second is the Anharmonic-Harmonic (AH-H) model considering anharmonic effect merely in the calculation of dissociation rate constant. In other words, we use anharmonic dissociation rate constants and harmonic isomerization rate constants to calculate the branching ratio. In the third model, the Anharmonic-Anharmonic (AH-AH) model, both the dissociation and isomerization rates adopt the values under anharmonic models. By this means, the energy dependences of

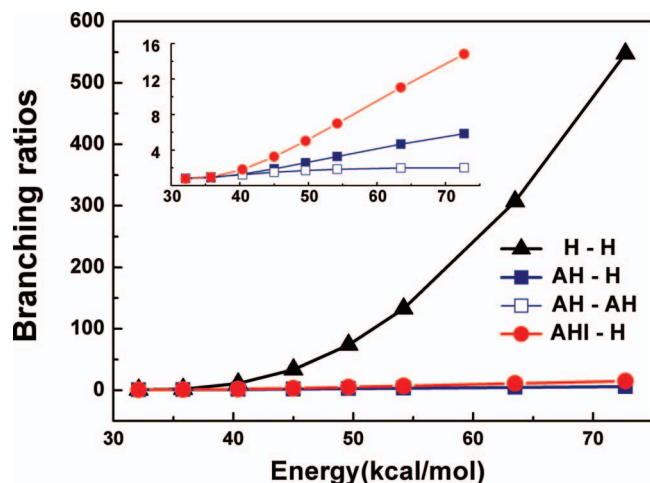


FIG. 4. The energy dependence of product branching ratios of $[\text{HD}_2\text{O}^+]/[\text{H}_2\text{DO}^+]$ under various kinetics models. An enlarged view of branching ratios under the AH-H, AH-AH, and AHI-H models as a function of energy is shown in the inset.

branching ratios $[\text{HD}_2\text{O}^+]/[\text{H}_2\text{DO}^+]$ under the H-H, AH-H, and AH-AH models were calculated and the results are plotted in Figure 4.

As shown in Figure 4, there is almost no discernible difference in the calculated values among the three models near the dissociation threshold around 31 kcal/mol. For instance, the branching ratios $[\text{HD}_2\text{O}^+]/[\text{H}_2\text{DO}^+]$ calculated by using the H-H, AH-H, and AH-AH models are separately 0.72, 0.79, and 0.84 at the energy of 32.1 kcal/mol. These results all consist with the experimental observation that branching ratios of $[\text{HD}_2\text{O}^+]/[\text{H}_2\text{DO}^+]$ are close to 1 at low collision energies.¹⁵ Thus, in the low energy range (below 40 kcal/mol), calculated branching ratios are not sensitive to whether the anharmonic effect is introduced into the kinetics model. Nevertheless, the results under the three models become considerably different when the total energy increases. In the energy range 40–73 kcal/mol, the branching ratios under the H-H model rapidly increase to 548 as shown in Figure 4, which are greatly deviated from experimental observations¹⁵ that branching ratios of HD_2O^+ to H_2DO^+ only went up from 1 to about 20 or 30 in the same energy range. Furthermore, at high total energy range, the predicted branching ratio as high as 548 would mean that the formation of H_2DO^+ can be completely ignored, but H_2DO^+ was clearly observed in the experiments.^{13,15} The contradictions between the prediction of H-H model and experimental results suggest that it is unreasonable to use the H-H model for calculating branching ratios in high total energy range.

From Figure 4, it is also seen that branching ratios predicted by AH-H and AH-AH models both fall into a reasonable range as anharmonic effect is considered. An enlarged view of the energy dependence of the results under the two models is shown in the inset of Figure 4. For the AH-H model, branching ratios are found to increase gradually from 1 to 6 with the growth of total energy, which are much closer to experimental results¹⁵ than those under H-H model. The more reasonable results obtained under AH-H model confirm further that proper dissociation rate constant

can be obtained only when anharmonic effect is considered. In fact, much smaller anharmonic dissociation rates instead of harmonic rates are used in the AH-H model, which reduces branching ratios to a reasonable range. However, as anharmonic effect is simultaneously included in describing both the dissociation and isomerization processes, branching ratios under the AH-AH model maintain a constant value of ~ 2 in the energy range from 40 to 73 kcal/mol as shown in the inset of Figure 4, which is apparently in contradiction with the experimentally observed gradual increase of branching ratio $[\text{HD}_2\text{O}^+]/[\text{H}_2\text{DO}^+]$ with the collision energy.

The quite different results obtained by the AH-H and AH-AH models imply that the anharmonic effect displayed with isomerization and dissociation is different. In the AH-AH model when isomerization is also treated with anharmonic approximation, the isomerization rate constants grow as the total energy increases, with similar amplitude to that of the dissociation rate constants (Figure 3). As a result, this leads to branching ratio predicted by the AH-AH model being no longer sensitive to the energy and remains at ~ 2 in a wide energy range. In the AH-H model, the increasing amplitude of harmonic isomerization rate with total energy is smaller than that of anharmonic dissociation rate. Consequently, branching ratios obtained by the AH-H model gradually rise with the growth of the energy, which agrees well with experimental results. Thus, the energy dependence of branching ratios predicted under the AH-H model is more reasonable. Overall, it shows that for the partially deuterated protonated water dimers, anharmonic oscillator with Morse potential is more suitable for calculating the dissociation rate, while harmonic approximation tends to be appropriate for calculating isomerization rate. This is reasonable if considering the characteristic PES of dissociation and isomerization, i.e., the geometry moves far away from the equilibrium position along the PES as the bond breaks, whereas the isomerization only occurs near the equilibrium position of the PES. Thus, the branching ratios of $[\text{HD}_2\text{O}^+]/[\text{H}_2\text{DO}^+]$ can be rationalized under the AH-H model. To improve this model further, the dissociation rate constants calculated under the anharmonic (Morse oscillator) model with free or hindered internal rotations treatment (Table S3 in the supplementary material³³) are applied in calculating the product branching ratios, and labeled as AHI-H model. The calculated branching ratios under AHI-H model are also plotted in Figure 4. It shows that the branching ratios under the AHI-H model gradually increase from 1 to about 15 in the given energy range, which agrees even better with the experimental results¹⁵ than those under the AH-H model, as expected.

IV. CONCLUSIONS

Partially deuterated protonated water dimers, $\text{H}_2\text{O} \cdot \text{H}^+ \cdot \text{D}_2\text{O}$, $\text{H}_2\text{O} \cdot \text{D}^+ \cdot \text{HDO}$, and $\text{HDO} \cdot \text{H}^+ \cdot \text{HDO}$, are important intermediates of the isotopic labeled reaction of $\text{H}_3\text{O}^+ + \text{D}_2\text{O}$. The isotope labeling reaction that involves dissociation and isomerization of these intermediates provides a physical picture for the proton migration during the symmetric exchange between two water molecules,

and invokes another type of important reaction, isotope scrambling.

We have investigated the dissociation and isomerization kinetics of partially deuterated protonated water dimers, $\text{H}_2\text{O} \cdot \text{H}^+ \cdot \text{D}_2\text{O}$, $\text{H}_2\text{O} \cdot \text{D}^+ \cdot \text{HDO}$, and $\text{HDO} \cdot \text{H}^+ \cdot \text{HDO}$, based on the harmonic and anharmonic oscillator models using RRKM theory and *ab initio* calculations. For the dissociation reaction, we find that the anharmonic and harmonic rate constants are quite different when the total energy increases, and the rate constants even become unreasonably large under the harmonic oscillator model in the high energy. This is an indication that the anharmonicity plays important roles affecting the dissociation of $\text{H}_2\text{O} \cdot \text{H}^+ \cdot \text{D}_2\text{O}$, $\text{H}_2\text{O} \cdot \text{D}^+ \cdot \text{HDO}$, and $\text{HDO} \cdot \text{H}^+ \cdot \text{HDO}$. However, for the isomerization reaction, anharmonic rate constants are only two to five times as large as harmonic results in the high energy range, implying that isomerization rates are insensitive to whether anharmonic or harmonic oscillator model is being applied.

On the basis of the calculated dissociation and isomerization rate constants, the branching ratios of two primary products, $[\text{HD}_2\text{O}^+]/[\text{H}_2\text{DO}^+]$, as a function of the energy are predicted under three kinetics models, the H-H, AH-H, and AH-AH models, respectively. The AH-AH model predicts that branching ratios maintain constantly at ~ 2 in the energy range from 40 to 73 kcal/mol. The branching ratios obtained with the AH-H model are found to increase gradually from 1 to 6 in the given energy range. More differently, for the H-H model, branching ratios are found to increase rapidly from 1 to 548 with the growth of total energy. AH-H model is shown to be a feasible kinetics model here for predicting branching ratios in agreement with experimental results, in which anharmonic dissociation and harmonic isomerization rate constants are used. This indicates that anharmonic oscillator with Morse potential is more suitable for calculating the dissociation rate, while harmonic approximation tends to be appropriate for calculating isomerization rates of this type of systems. To further improve AH-H model, the three low frequency vibrations below 100 cm^{-1} of the dissociation transition states are separately treated with free or hindered internal rotations, while other frequency vibrations treated with the anharmonic (Morse oscillator) model and the computed dissociation rate constants are applied in calculating the product branching ratios (AHI-H model). It shows that the branching ratios under the AHI-H model gradually increase from 1 to about 15 in the given energy range, which agrees even better with the experimental results than those under the AH-H model, as expected. Overall, the anharmonic RRKM calculations provide a rationale for the energy dependence experimentally observed with the product branching ratios of proton transfer versus isotope scrambling.

ACKNOWLEDGMENTS

This work was supported by the National Natural Science Foundation of China (Grant Nos. 21073201 and 21003134), the National Basic Research Program of China (Grant No. 2013CB834602), the water science project of Chinese Academy of Sciences, and the National Sciences Council of Taiwan.

- ¹L. I. Yeh, M. Okumura, J. D. Myers, J. M. Price, and Y. T. Lee, *J. Chem. Phys.* **91**, 7319 (1989).
- ²C. Lao-ngam, P. Asawakun, S. Wannarat, and K. Sagarik, *Phys. Chem. Chem. Phys.* **13**, 4562 (2011).
- ³R. Vuilleumier and D. Borgis, *J. Phys. Chem. B* **102**, 4261 (1998).
- ⁴C. Knight and G. A. Voth, *Acc. Chem. Res.* **45**, 101 (2012).
- ⁵F. Garczarek and K. Gerwert, *Nature (London)* **439**, 109 (2006).
- ⁶R. Parthasarathi, V. Subramanian, and N. Sathyamurthy, *J. Phys. Chem. A* **111**, 13287 (2007).
- ⁷N. Agmon, *Chem. Phys. Lett.* **244**, 456 (1995).
- ⁸D. Marx, M. E. Tuckerman, J. Hutter, and M. Parinello, *Nature (London)* **397**, 601 (1999).
- ⁹K. R. Asmis, N. L. Pivonka, G. Santambrogio, M. Brümmer, C. Kaposta, D. M. Neumark, and L. Wöste, *Science* **299**, 1375 (2003).
- ¹⁰T. D. Fridgen, T. B. McMahon, L. MacAleese, J. Lemaire, and P. Maitre, *J. Phys. Chem. A* **108**, 9008 (2004).
- ¹¹T. L. Guasco and M. A. Johnson, *J. Phys. Chem. A* **115**, 5847 (2011).
- ¹²J. Rheinecker, T. Xie, and J. M. Bowman, *J. Chem. Phys.* **120**, 7018 (2004).
- ¹³P. W. Ryan, C. R. Blakey, M. L. Vestal, and J. H. Futrell, *J. Phys. Chem.* **84**, 561 (1980).
- ¹⁴D. Song, H. Su, F. Kong, and S. H. Lin, *J. Phys. Chem. A* **114**, 10217 (2010).
- ¹⁵K. Honma and P. B. Armentrout, *J. Chem. Phys.* **121**, 8307 (2004).
- ¹⁶T. Beyer and D. F. Swinehart, *Commun. Assoc. Comput. Mach.* **16**, 379 (1973).
- ¹⁷K. Song and W. L. Hase, *J. Chem. Phys.* **110**, 6198 (1999).
- ¹⁸L. Yao, A. M. Mebel, and S. H. Lin, *J. Phys. Chem. A* **113**, 14664 (2009).
- ¹⁹L. Yao, A. M. Mebel, H. F. Lu, H. J. Neusser, and S. H. Lin, *J. Phys. Chem. A* **111**, 6722 (2007).
- ²⁰L. Yao, R. X. He, A. M. Mebel, and S. H. Lin, *Chem. Phys. Lett.* **470**, 210 (2009).
- ²¹G. M. Chaban, J. O. Jung, and R. B. Gerber, *J. Phys. Chem. A* **104**, 2772 (2000).
- ²²M. V. Vener, O. Kühn, and J. Sauer, *J. Chem. Phys.* **114**, 240 (2001).
- ²³J. E. Del Bene and M. J. T. Jordan, *J. Chem. Phys.* **108**, 3205 (1998).
- ²⁴S. H. Lin, *J. Chem. Phys.* **65**, 1053 (1976); M. Hayashi, Y. J. Shiu, K. K. Liang, S. H. Lin, and Y. R. Shen, *J. Phys. Chem. A* **111**, 9062 (2007).
- ²⁵V. Barone, *J. Chem. Phys.* **120**, 3059 (2004); **122**, 014108 (2005).
- ²⁶J. M. Bowman, *J. Chem. Phys.* **68**, 608 (1978); *Acc. Chem. Res.* **19**, 202 (1986).
- ²⁷A. Ratner and R. B. Gerber, *J. Phys. Chem.* **90**, 20 (1986).
- ²⁸M. J. Frisch, G. W. Trucks, H. B. Schlegel *et al.*, GAUSSIAN 03, Revision B.03, Gaussian, Inc., Wallingford, CT, 2004.
- ²⁹V. V. Kislova, T. L. Nguyen, A. M. Mebel, S. H. Lin, and S. C. Smith, *J. Chem. Phys.* **120**, 7008 (2004).
- ³⁰E. M. Evleth, Z. D. Hamou-Tahra, and E. Kassab, *J. Phys. Chem.* **95**, 1213 (1991).
- ³¹M. Meot-Ner and C. V. Speller, *J. Phys. Chem.* **90**, 6616 (1986).
- ³²A. J. Cunningham, J. D. Payzant, and P. Kebarle, *J. Am. Chem. Soc.* **94**, 7627 (1972).
- ³³See supplementary material at <http://dx.doi.org/10.1063/1.4794152> for the values of dissociation rate constants and isomerization rate constants.
- ³⁴D. T. Colbert and W. H. Miller, *J. Chem. Phys.* **96**, 1982 (1992).